



Magnetic resonance elastography for noninvasive detection of liver fibrosis: is there an added value of 3D acquisition?

Enamul H. Bhuiyan^{1,2} · Efe Ozkaya^{1,2} · Paul Kennedy^{1,2} · Juan Lloret Del Hoyo^{2,3} · Bassam El Achkar² · Swan Thung⁴ · Sara Lewis^{1,2} · Octavia Bane^{1,2} · Bachir Taouli^{1,2}

Received: 2 May 2023 / Revised: 22 August 2023 / Accepted: 24 August 2023 / Published online: 12 September 2023
© The Author(s), under exclusive licence to Springer Science+Business Media, LLC, part of Springer Nature 2023

Abstract

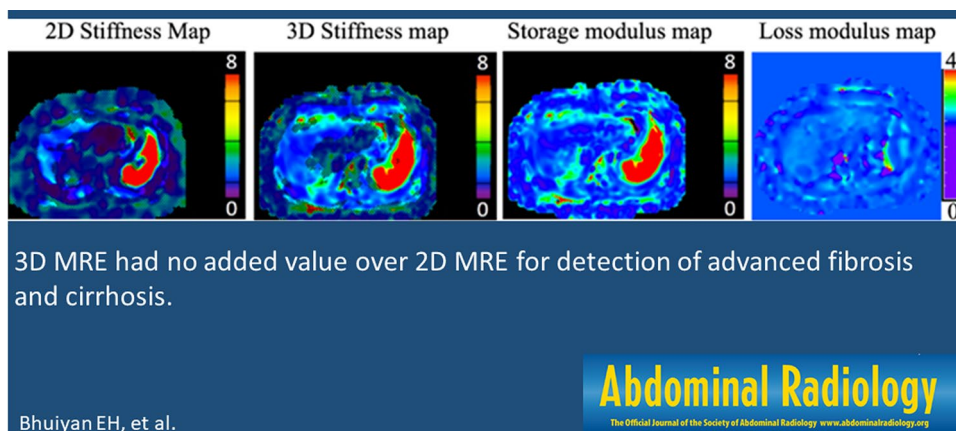
Purpose (1) Assess the diagnostic performance of liver 3D magnetic resonance elastography (MRE) parameters (including stiffness, storage/loss modulus and damping ratio) compared to liver stiffness measured with 2D MRE for noninvasive detection of advanced liver fibrosis (F3-F4) and cirrhosis (F4) in patients with chronic liver disease. (2) Assess the value of serum markers (FIB-4) in detecting advanced liver fibrosis and cirrhosis in the same patients.

Methods This was a single center, prospective IRB-approved cross-sectional study that included 49 patients (M/F: 23/26, mean age 50.8 y) with chronic liver disease and concomitant liver biopsy. MRE was acquired at 1.5T using a spin echo-EPI sequence. The following parameters were measured: liver stiffness using 2D MRE (LS-2D) and 3D MRE parameters (LS-3D, liver storage, loss modulus and damping ratio). The Mann-Whitney U test, ROC curve analysis, Spearman correlation and logistic regression were performed to evaluate diagnostic performance of MRE parameters and FIB-4.

Results LS-2D and LS-3D had similar diagnostic performance for diagnosis of F3-F4, with AUCs of 0.87 and 0.88, sensitivity of 0.71 and 0.81, specificity of 0.89 for both. For diagnosis of F4, LS-2D and LS-3D had similar performance with AUCs of 0.81 for both, sensitivity of 0.75 and 0.83, and specificity of 0.84 and 0.73, respectively. Additional 3D parameters (storage modulus, loss modulus, damping ratio) had variable performance, with AUC range of 0.59-0.78 for F3-F4; and 0.52-0.70 for F4. FIB-4 had lower diagnostic performance, with AUCs of 0.66 for F3-F4, and 0.68 for F4.

Conclusion Our study shows no added value of 3D MRE compared to 2D MRE for detection of advanced fibrosis and cirrhosis, while FIB-4 had lower diagnostic performance.

Graphical abstract



Keywords Magnetic resonance elastography · Liver fibrosis · Liver stiffness

Extended author information available on the last page of the article

Introduction

Noninvasive staging of liver fibrosis in patients with chronic liver disease (CLD) is essential for patient management and for assessment of prognosis, and has largely replaced liver biopsy in clinical practice [1]. Patients with cirrhosis require assessment of risk of portal hypertension and screening for hepatocellular carcinoma (HCC) [2]. Various noninvasive methods to detect liver fibrosis have been developed over the past two decades. These include blood tests, ultrasound elastography (including transient elastography and shear wave elastography), and magnetic resonance elastography (MRE). Ultrasound elastography and shear wave elastography can fail or provide unreliable measurements in patients who are overweight or obese [3] MRE is considered an accurate and reliable method for predicting liver fibrosis stage based on liver stiffness measurement, however, is limited by cost and availability [4–9]. MRE involves processing the transverse component of the wave field (shear wave) data using generally a 2D-inversion algorithm to generate quantitative images of liver stiffness, also known as elastograms. Earlier versions of 2D MRE were acquired using gradient recalled echo (GRE) sequences [10], which has shown excellent diagnostic performance in staging liver fibrosis [11–14]. Recently, there has been increased use of spin echo echo-planar imaging (SE-EPI) for MRE acquisition, particularly at 3T, to reduce the risk of technical failure (for example caused by iron deposition) [5, 15–22]. The more recent technique, 3D MRE, quantifies stiffness in 3 directions of wave propagation instead of only one direction perpendicular to the imaging slices. 3D MRE typically uses a multislice SE-EPI sequence, with a study suggesting better image quality and larger volume coverage compared to 2D MRE [23]. One of the advantages of 3D MRE is the extended multislice coverage (26 slices) of the liver compared to 2D-MRE (10 slices), and the provision of additional tissue markers, such as the individual components of the complex shear modulus, which may add value to liver stiffness [24]. However, different MRE methods may produce different liver stiffness values [25]. Previous studies comparing 2D and 3D MRE did not find added value of 3D MRE for liver fibrosis detection [8, 13, 15, 25–31]. A study in patients with HBV and HCV showed that liver damping ratio and shear stiffness were able to identify necroinflammation in the early stages of the disease to differentiate it from fibrosis. However, none of these previous studies assessed liver storage and loss modulus from 3D MRE separately for fibrosis staging.

Our study objectives are to: (1) Assess the diagnostic performance of liver 3D MRE parameters (including stiffness, storage/loss modulus and damping ratio) compared

to liver stiffness measured with 2D MRE for noninvasive detection of advanced liver fibrosis and cirrhosis in patients with CLD. (2) Assess the value of serum markers (FIB-4) in detecting advanced liver fibrosis and cirrhosis in the same patients.

Materials and methods

This is an IRB-approved single-center prospective study involving patients with CLD and suspected portal hypertension who underwent a clinically indicated hepatic venous pressure gradient measurement with a transjugular liver biopsy, and a research MRI. All patients provided signed informed consent. Forty patients were included in a previously published study, in which assessing fibrosis detection was not the main objective [3].

Inclusion and exclusion criteria

Inclusion criteria were: patients with CLD (including all etiologies of liver disease), age ≥ 18 y, clinically indicated transjugular liver biopsy within 3 months of the MRI study.

Exclusion criteria were: previous liver transplant and contra-indications to MRI. The study involved 55 patients, of whom 6 were excluded (see patient flowchart in Fig. 1). The patients' characteristics are listed in Table 1.

MRE acquisition

All patients underwent 2D and 3D SE-EPI MRE examinations during the same MRI study, as part of a multiparametric liver MRI protocol that also included T₁ mapping, 4D flow imaging and dynamic contrast-enhanced MRI. The results from the other MRI sequences are not reported in this study. All MRE examinations were conducted using a 1.5T system (Magnetom Aera, Siemens Healthineers, Erlangen,

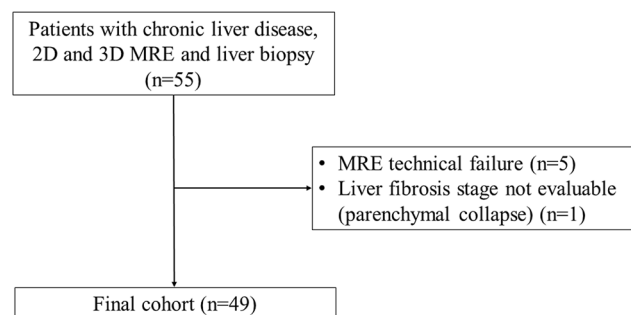


Fig. 1 Patient flowchart

Table 1 Study cohort characteristics (n = 49)

Demographics	
Sex (M/F)	23/26
Age (years), mean \pm SD (range)	50.8 \pm 15.6 (19–78)
Etiology	
Nonalcoholic steatohepatitis (NASH)	13
Alcohol intoxication	9
Primary sclerosing cholangitis (PSC)	5
Autoimmune hepatitis	5
Drug induced liver injury	4
Obliterative portal venopathy	3
Primary biliary cholangitis	1
Other*	9
Blood tests	
FIB-4, mean \pm SD (range)	3.0 \pm 2.6 (0.2–11.6)
Fibrosis stage	
F0/F1/F2/F3/F4	10/10/9/8/12
Collagen proportionate area (CPA), mean \pm SD (range)	0.22 \pm 0.16 (0.02–0.61)
Interval between MRE and biopsy, mean \pm SD (range) days	33.2 \pm 21.4 (1.0–102.0)
Interval between MRE and FIB-4, mean \pm SD (range) days	31.9 \pm 26.7 (0–111.0)

*Other: mastocytosis, cryptogenic liver disease, hemochromatosis, non-specific reactive hepatitis, granulomatous hepatitis.

SD standard deviation

Germany) with an 8-channel, phased-array, torso coil. A passive pneumatic drum was placed on the right side and left side over the spleen for dual actuation using mechanical vibrations at 60Hz [32]. Two MRE protocols were used: the 2D SE-EPI MRE protocol acquired 10 axial slices in a single breath-hold, whereas the 3D SE-EPI MRE protocol acquired 32 axial slices in 3 breath-holds. Only the liver related MRE results are presented in this study. The sequence parameters of the 2D and 3D MRE exams are summarized in Table 2.

Image analysis

Two observers (observer 1, XX and observer 2, XX, both medical physicists, with 8 and 5 years of experience, respectively) drew regions of interest (ROIs) on MRE magnitude, wave, and elastogram images overlaid with confidence maps on the right hepatic lobe, using Fiji (ImageJ). The dataset was equally divided between observers. Four consecutive central slices spanning the widest part of the liver were selected from the 10 slices acquired in 2D MRE, while 4 slices were selected from the 32-transverse sections of the 3D MRE examination to match the 2D MRE selected slices. On magnitude images, the observers drew ROIs on the largest possible area of the liver parenchyma where coherent shear waves were visible and major blood vessels

were excluded. Areas of incoherent waves were avoided and regions immediately under the passive driver and areas close to the liver boundary were excluded, so that the final ROI selection contained a minimum of 500 pixels per slice [33, 34]. After drawing ROIs, the observers recorded the mean liver stiffness in 2D (LS-2D) and 3D MRE (LS-3D), as well as storage and loss modulus in 3D MRE of each section and computed and weighed the mean value of all sections by ROI size. The damping ratio was calculated as the ratio of the loss modulus to two times the storage modulus [29, 31, 35].

Histopathologic assessment

All patients underwent a transjugular liver biopsy within 33 \pm 21 days of MRI that was evaluated retrospectively by an experienced liver pathologist who was blinded to the patients' laboratory and imaging data. Liver fibrosis was scored on a five-point scale using the METAVIR [36, 37] scoring system for all etiologies except for NASH, where the NASH-CRN score was used [38]. The fibrosis stage was assigned using an ordinal scale from 0 to 4: F0: no fibrosis, F1: mild fibrosis, F2: moderate fibrosis, F3: advanced fibrosis, F4: cirrhosis. In addition, quantification of liver collagen proportionate areas (CPA) was performed

Table 2 2D and 3D MRE acquisition parameters

Parameters	2D MRE	3D MRE
Sequence	Spin echo-EPI	Spin echo-EPI
Acquisition matrix	100–100	100–100
Standard shear-wave frequency	60 Hz	60 Hz
TE (ms)	41	40
TR (ms)	1500	3200
Flip angle (degree)	90	90
EPI-shots	1	1
No. of breath holds × breath hold time (s)	1–15	3–17
FOV (mm)	380–400	380–440
No. of slices × slice thickness (mm)	10–5	26–3.5
Gap between slices (mm)	4.5	3.5
Parallel imaging acceleration factor	2	2
Phase offsets	4	4
Receiver bandwidth	500 kHz	500 kHz
% FOV in phase-encoding direction	65–100	100
Superior-inferior spatial pre-saturation bands	Yes	Yes
Flow compensation	Yes	Yes
Motion sensitivity (μm/radian)	7.86	7.86
Motion encoding directions	±Z	±X, Y, Z

TE echo time, *TR* repetition time, *FOV* field of view, *2D* two-dimensional, *3D* three-dimensional, *EPI* echo-planar imaging, *MRE* magnetic resonance elastography

using picrosirius red staining to measure collagen content in the biopsy samples [39] and correlate it with liver parameters measured by 2D and 3D MRE.

Study endpoints

The endpoints were detection of advanced fibrosis (F3-F4) and cirrhosis (F4).

Statistical analysis

The Mann-Whitney *U*-test was used to analyze the differences in LS measured with 2D and 3D MRE, storage modulus, loss modulus and damping ratio between patients stratified as F0-F2 vs F3-F4 and F0-F3 vs F4. We assessed the correlation between MRE parameters and CPA, and the diagnostic performance of 2D MRE, 3D MRE and FIB-4 for detecting F3-F4 and F4 using ROC curve analyses. We also performed binary logistic regression combining the statistically significant parameters. The statistical analyses were performed using SPSS (version 26, IBM) and MATLAB 2020 (MATLAB Nautick). A *p*-value less than 0.05 was considered statistically significant.

Results

The final population included 49 patients, of which 20 had stage F3-F4 (advanced fibrosis) and 12 had F4 (cirrhosis). Table 1 summarizes the cohort information.

Performance of 2D MRE, 3D MRE, and FIB-4

The LS values obtained with 2D and 3D MRE scans were strongly correlated with each other ($r = 0.82$, $p < 0.001$), though 3D (mean \pm SD: 2.9 ± 1.1 kPa for F3-F4 and 3.6 ± 2.0 kPa for F4) values were generally lower ($p < 0.001$) than 2D values (mean \pm SD: 3.4 ± 1.1 kPa for F3-F4 and 4.1 ± 2.1 kPa for F4) (Tables 3 and 4). The distribution of LS values showed a separation of F0-F2 from F3-F4, and from F0-F3 from F4, while there was more overlap between groups for storage modulus, loss modulus and damping ratio (Figs. 2, 3 and 4). ROC analysis for diagnosing F3-F4 (Table 3) and F4 (Table 4) showed very good performance of LS-2D (AUCs of 0.87 [confidence intervals: 0.77–0.97] and 0.81 [0.68–0.95]) and LS-3D (AUCs 0.88 [0.77–0.98] and 0.81 [0.67–0.95]). Storage, loss modulus and damping ratio had variable performance, with storage modulus having the best performance, with

Table 3 Diagnostic performance of MRE parameters and FIB-4 for detection of advanced liver fibrosis and cirrhosis (F3-F4)

Parameter	F0–F2 (n = 28)	F3–F4 (n = 21)	p*	AUC [95% CI]	p**	Sensitivity	Specificity	Cutoff value
LS-2D (kPa)	3.47 ± 1.16	6.70 ± 3.44	<0.001	0.87 [0.77–0.97]	<0.001	0.71	0.89	4.23
LS-3D (kPa)	2.96 ± 1.10	6.08 ± 2.87	<0.001	0.88 [0.77–0.98]	<0.001	0.81	0.89	3.82
Storage modulus (kPa)	3.15 ± 1.17	5.77 ± 3.85	0.001	0.78 [0.64–0.92]	0.001	0.75	0.81	3.70
Loss modulus (kPa)	1.42 ± 0.71	1.52 ± 0.55	0.298	0.59 [0.42–0.76]	0.298	0.90	0.38	0.85
Damping ratio	0.24 ± 0.14	0.18 ± 0.13	0.138	0.63 [0.46–0.80]	0.138	0.77	0.55	0.12
FIB-4	2.63 ± 2.67	3.70 ± 2.52	0.057	0.66 [0.51–0.82]	0.057	0.85	0.46	1.61

AUC area under the curve, CI confidence intervals, LS-2D 2D liver stiffness, LS-3D 3D liver stiffness

p*: Mann-Whitney test, p**: for AUC

Table 4 Diagnostic performance of MRE parameters and FIB-4 for detection of cirrhosis (F4)

Parameters	F0–F3 (n = 37)	F4 (n = 12)	p*	AUC [95% CI]	p**	Sensitivity	Specificity	Cutoff value
LS-2D (kPa)	4.1 ± 2.1	7.0 ± 3.7	0.001	0.81 [0.68–0.95]	0.001	0.75	0.84	5.2
LS-3D (kPa)	3.6 ± 2.0	6.2 ± 2.9	0.001	0.81 [0.67–0.95]	0.001	0.83	0.73	3.8
Storage modulus (kPa)	3.7 ± 2.2	6.0 ± 4.1	0.043	0.70 [0.49–0.92]	0.043	0.73	0.83	4.4
Loss modulus (kPa)	1.46 ± 0.6	1.48 ± 0.45	0.879	0.52 [0.34–0.70]	0.867	0.91	0.37	1.0
Damping ratio	0.23 ± 0.14	0.18 ± 0.16	0.261	0.62 [0.41–0.82]	0.252	0.71	0.64	0.12
FIB-4	2.7 ± 2.6	3.9 ± 2.4	0.061	0.68 [0.52–0.85]	0.061	0.65	0.35	1.4

AUC area under the curve, CI confidence intervals, LS-2D 2D liver stiffness, LS-3D 3D liver stiffness

p*: Mann-Whitney test, p**: for AUC

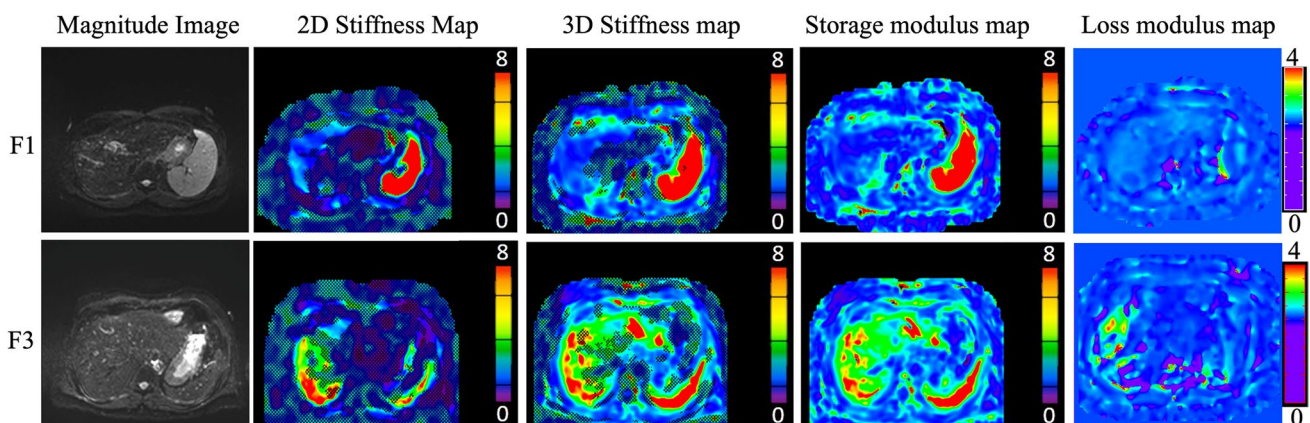


Fig. 2 Top row: 39-year-old male with obliterative portal venopathy and stage F1 (mild fibrosis). Liver stiffness values with 2D, 3D MRE, storage, loss modulus and damping ratio were 2.71 kPa, 2.46 kPa, 2.39 kPa, 2.11 kPa and 0.44, respectively. Bottom row: 48-year-old

male with alcohol-related liver disease and stage F3 (advanced fibrosis). Liver stiffness values with 2D, 3D MRE, storage, loss modulus and damping ratio were 5.82 kPa, 5.85 kPa, 5.68 kPa, 2.18 kPa and 0.19, respectively

AUCs of 0.78 [0.64–0.92] for F3-F4 and 0.70 [0.49–0.92] for F4. FIB-4 had lower performance, with AUC of 0.66 [0.51–0.82] for F3-F4 and 0.68 [0.52–0.85] for F4 (Tables 3 and 4). The combination of multiple significant parameters using binary logistic regression did not improve performance over LS alone (maximum AUCs of 0.88 [0.77–0.98] and 0.81 [0.67–0.95] for F3-F4 and F4, respectively).

Correlation with CPA

The Spearman correlations between MRE parameters and CPA are summarized in Table 5. LS-2D ($r = 0.30$, $p = 0.039$), LS-3D ($r = 0.45$, $p = 0.002$) and loss modulus ($r = 0.50$, $p = 0.001$) showed significant weak to moderate positive correlations with CPA.

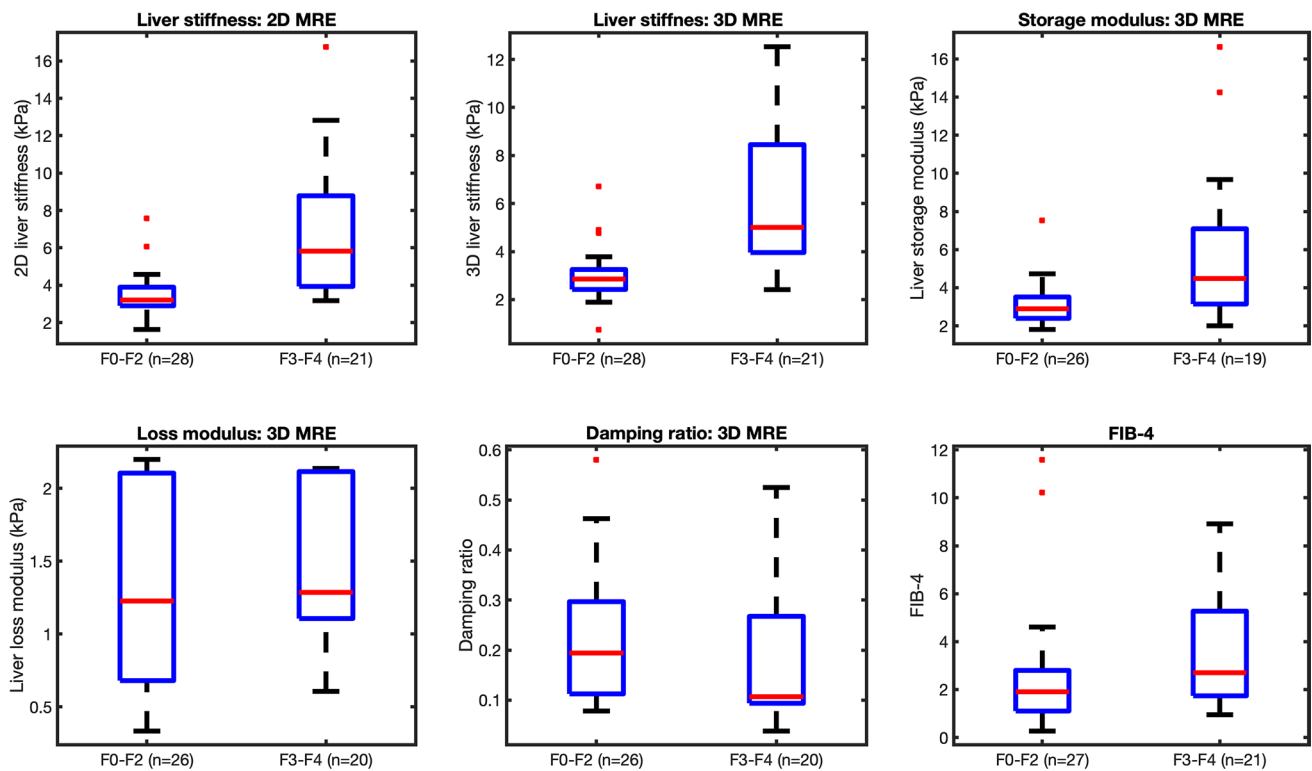


Fig. 3 Distribution of MRE parameters and FIB-4 values in patients stratified as F0-F2 vs F3-F4: **a** 2D liver stiffness, **b** 3D liver stiffness, **c** liver storage modulus, **d** liver loss modulus, **e** damping ratio, and **f**

FIB-4. Red line on the box plot represents median and the error bar represents 1.5x inter quartile range (IQR)

Discussion

Noninvasive detection of liver fibrosis in patients with CLD is an important clinical question, with elastography methods having largely replaced liver biopsy for liver fibrosis staging in the clinic. While LS-3D allows for improved assessment of spatial patterns of liver fibrosis, LS-2D is simpler to implement as shear wave is unidirectional. Though 3D MRE can evaluate a larger liver volume [25, 26], our study demonstrated that LS-2D and LS-3D performed equally well in diagnosing advanced fibrosis (F3-F4) and cirrhosis (F4), while FIB-4 had lower performance.

Our results indicate that, despite theoretical advantages, such as the potential for improved measurement accuracy, LS-3D did not outperform LS-2D in staging liver fibrosis. Both techniques showed very good performance (AUC = 0.81 – 0.88) in diagnosing advanced fibrosis/ cirrhosis or cirrhosis; consistent with previous studies [12, 25, 26, 32–34]. However, the performance in our study was in the lower end of performance based on what has been reported previously (AUC range for F3-F4 = 0.83 – 0.95 and F4 = 0.89 – 0.97) [40], which could be due to the mixed etiology of CLD. In our study, MRE outperformed FIB-4, consistent with a previous publication [41].

The (relative) wide availability and fast acquisition of the LS-2D technique justify its use in clinical practice for liver fibrosis staging. Similar to our findings, previous studies reported higher cutoff values for LS-2D vs LS-3D for staging advanced fibrosis and cirrhosis [25, 42]. This could be explained by the limited spatial coverage of 2D MRE, as it only captures mechanical wave images in a single slice of the liver. This can lead to sampling error and reduced accuracy in cases where there is significant heterogeneity in the liver's mechanical properties across different regions. In other words, 3D MRE offers several advantages over 2D MRE, reduced sampling error [10, 43, 44] and reduced susceptibility to motion artifact, although this was not evaluated in our study. However, LS measured with 3D MRE did not have added diagnostic value, as suggested in previous studies [8, 25, 27–29, 31]. It is possible to perform 3D MRE in lower frequency and at a lower shear wave frequency of 40 Hz which may provide improved diagnostic performance [25]. This could be the subject of additional studies.

CPA positively correlated with LS-2D and with LS-3D, whereas it positively correlated with liver loss modulus. Besides LS, the parameters derived from 3D MRE (liver storage, loss modulus and damping ratio) had lower diagnostic performance for advanced fibrosis (AUC = 0.59 – 0.78)

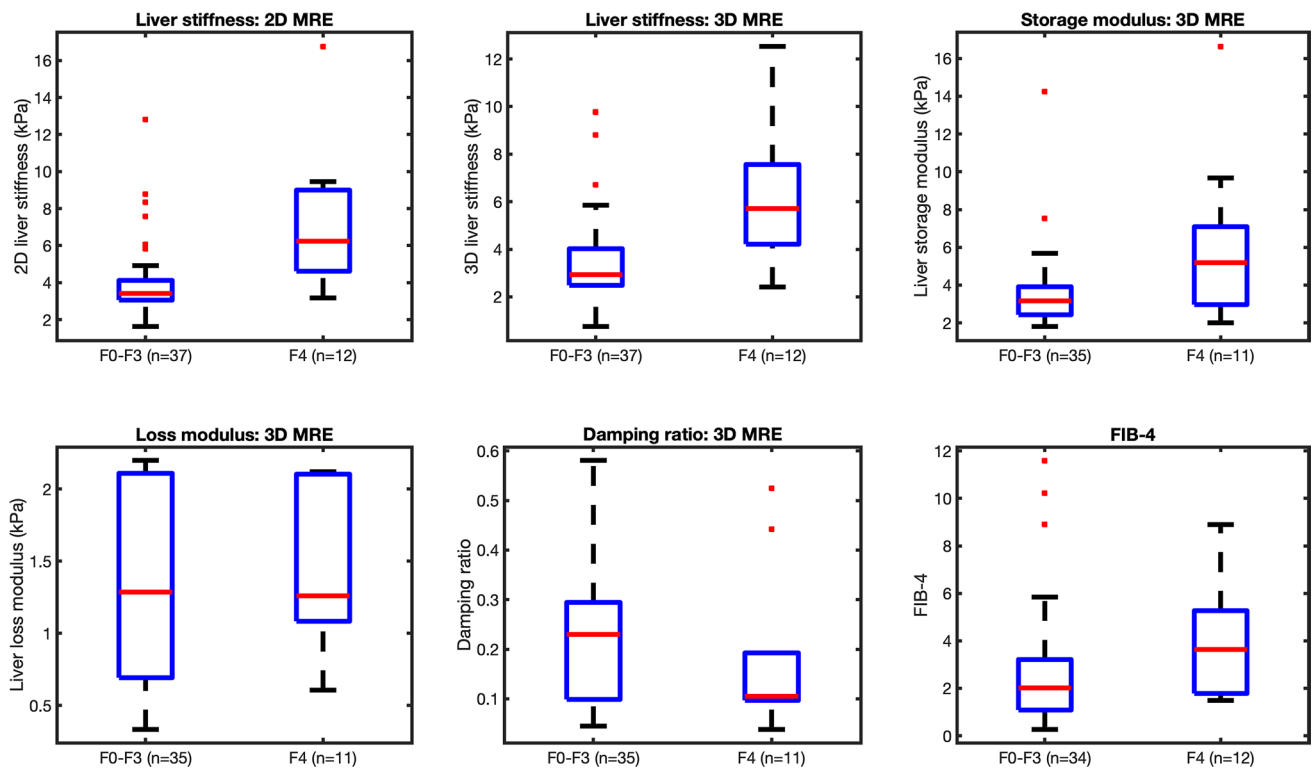


Fig. 4 Distribution of MRE parameters and FIB-4 values in patients stratified as F0-F3 vs F4: **a** 2D liver stiffness, **b** 3D liver stiffness, **c** liver storage modulus, **d** liver loss modulus, **e** damping ratio, and **f**

FIB-4. Red line on the box plot represents median and the error bar represents 1.5x inter quartile range (IQR)

Table 5 Spearman correlation results between MRE parameters and CPA

Parameters		LS-2D	LS-3D	Storage modulus	Loss modulus	Damping ratio
CPA	r (p)	0.301 (0.039)	0.450 (0.002)	0.224 (0.144)	0.498 (0.001)	0.235 (0.124)
LS-2D	r (p)		0.825 (< 0.001)	0.649 (< 0.001)	-0.061 (0.689)	-0.505 (<0.001)
LS-3D	r (p)			0.772 (<0.001)	0.191 (0.204)	-0.367 (0.012)
Storage modulus	r (p)				0.160 (0.288)	-0.563 (<0.001)
Loss modulus	r (p)					0.669 (<0.001)

CPA collagen proportionate areas, LS-2D 2D liver stiffness, LS-3D 3D liver stiffness.

r = Spearman rank correlation coefficient

and cirrhosis (AUC = 0.52 – 0.70), and thus did not have added value for fibrosis staging.

The storage modulus measures the liver tissue's elasticity and its ability to store energy when it is deformed, while the loss modulus measures tissue viscosity and the ability to dissipate energy when deformed. As fibrosis progresses in the liver, the tissue's viscosity decreases while its stiffness increases. This leads to alterations in both the storage and loss moduli. To capture these changes, the absolute value of the complex shear modulus is used, which is represented through elastograms. Elastogram incorporates information obtained from storage and loss moduli combined, instead of focusing on one parameter alone (either storage or loss)

causing the moduli parameters to have lower AUCs than the stiffness parameter.

Our study has a few limitations: (1) the sample size was limited due to strict inclusion/exclusion criteria, (2) we included a population with varied etiologies, which may have introduced bias. To validate our current results, studies enrolling patients with single etiology CLD should be performed.

In conclusion, our study showed no added value of 3D MRE parameters compared to 2D MRE for the detection of advanced fibrosis and cirrhosis, with LS measured with both techniques having similar and very good performance, superior to FIB-4 for liver fibrosis staging.

Acknowledgements None.

Funding This work was supported by NIDDK, Grant No. R01DK113272.

Data availability The main data that support this study are available within the paper. All other experimental data are available upon request, by contacting the corresponding author.

Declarations

Conflict of interest No conflict of interest.

References


- Kennedy P, Wagner M, Castéra L, Hong CW, Johnson CL, Sirin CB, Taouli B. Quantitative Elastography Methods in Liver Disease: Current Evidence and Future Directions. *Radiology*. 2018;286(3):738–63. <https://doi.org/10.1148/radiol.2018170601>. PubMed PMID: 29461949; PMCID: PMC5831316.
- Castera L. Noninvasive methods to assess liver disease in patients with hepatitis B or C. *Gastroenterology*. 2012;142(6):1293–302; PMCID: PubMed: 22537436.
- Kennedy P, Stocker D, Carbonell G, Said D, Bane O, Hectors S, Abboud G, Cuevas J, Bolster BD, Jr., Friedman SL, Lewis S, Schiano T, Bhattacharya D, Fischman A, Thung S, Taouli B. MR elastography outperforms shear wave elastography for the diagnosis of clinically significant portal hypertension. *Eur Radiol*. 2022;32(12):8339–49. Epub 20220621. <https://doi.org/10.1007/s00330-022-08935-9>. PubMed PMID: 35727321.
- Rustogi R, Horowitz J, Harmath C, Wang Y, Chalian H, Ganger DR, et al. Accuracy of MR elastography and anatomic MR imaging features in the diagnosis of severe hepatic fibrosis and cirrhosis. *J Magn Reson Imaging*. 2012;35(6):1356–64. <https://doi.org/10.1002/jmri.23585>.
- Singh S, Venkatesh SK, Wang Z, Miller FH, Motosugi U, Low RN, et al. Diagnostic performance of magnetic resonance elastography in staging liver fibrosis: a systematic review and meta-analysis of individual participant data. *Clin Gastroenterol Hepatol*. 2015;13(3):440–51. <https://doi.org/10.1016/j.cgh.2014.09.046>.
- Srinivasa B, A, Wells ML, Teytelboym OM, et al. Elastography in Chronic Liver Disease: Modalities, Techniques, Limitations, and Future Directions. *Radiographics*. 2016;36(7):1987–2006.
- Lefebvre T, Wartelle-Bladou C, Wong P et al. Prospective comparison of transient, point shear wave, and magnetic resonance elastography for staging liver fibrosis. *Eur Radiol*. 2019;29:6477–88. <https://doi.org/10.1007/s00330-019-06331-4>.
- Hoodeshenas S YM, Venkatesh SK. Magnetic resonance elastography of liver: current update. *Top Magn Reson Imaging* 2018;27:319–33. <https://doi.org/10.1097/RMR.0000000000000177>.
- Venkatesh SK YM, Ehman RL. Magnetic resonance elastography of liver: technique, analysis, and clinical applications. *J Magn Reson Imaging*. 2013;37(3):544–55. <https://doi.org/10.1002/jmri.23731>.
- Yin M TJ, Glaser KJ et al. Assessment of hepatic fibrosis with magnetic resonance elastography. *Clin Gastroenterol Hepatol*. 2007;5(10):1207–13. <https://doi.org/10.1016/j.cgh.2007.06.012>.
- Zhan C, Kannengiesser S, Chandarana H, Fenchel M, Ream J, Shanbhogue KP. MR elastography of liver at 3 Tesla: comparison of gradient-recalled echo (GRE) and spin-echo (SE) echo-planar imaging (EPI) sequences and agreement across stiffness measurements. *Abdom Radiol (NY)*. 2019;44:1825–33. <https://doi.org/10.1007/s00261-019-01932-5>.
- Shi Y, Xia F, Li QJ, et al. Magnetic resonance elastography for the evaluation of liver fibrosis in chronic hepatitis b and c by using both gradient-recalled echo and spin-echo echo planar imaging: a prospective study. *Am J Gastroenterol*. 2016;111:823–33. <https://doi.org/10.1038/ajg.2016.56>.
- Kim YS, Jang YN, Song JS. Comparison of gradient-recalled echo and spin-echo echo-planar imaging MR elastography in staging liver fibrosis: a meta-analysis. *Eur Radiol*. 2018;28(4):1709–18. <https://doi.org/10.1007/s00330-017-5149-5>.
- Chang W, Lee JM, Yoon JH, et al. Liver fibrosis staging with MR elastography: comparison of diagnostic performance between patients with chronic hepatitis b and those with other etiologic causes. *Radiology*. 2016;280(1):88–97. <https://doi.org/10.1148/radiol.2016150397>.
- Wang J, Glaser KJ, Zhang T et al. Assessment of advanced hepatic MR elastography methods for susceptibility artifact suppression in clinical patients. *J Magn Reson Imaging*. 2018;47(4):976–87. <https://doi.org/10.1002/jmri.25818>.
- Wagner M, Corcuera-Solano I, Lo G et al. Technical failure of MR elastography examinations of the liver: experience from a large Single-Center study. *Radiology*. 2017;284(2):401–12. <https://doi.org/10.1148/radiol.2016160863>.
- Felker ER, Choi KS, Sung K, et al Liver MR elastography at 3 T: agreement across pulse sequences and effect of liver R2* on image quality. *AJR Am J Roentgenol*. 2018;211(3):588–94. <https://doi.org/10.2214/AJR.17.19288>.
- Wagner M, Besa C, Bou AJ, et al. Magnetic resonance elastography of the liver: qualitative and quantitative comparison of gradient echo and spin echo echo-planar imaging sequences. *Invest Radiol*. 2016;51(9):575–81. <https://doi.org/10.1097/RLI.0000000000000269>.
- Mariappan YK, Dzyubak B, Glaser KJ, et al. Application of modified spin-echo-based sequences for hepatic MR elastography: evaluation, comparison with the conventional gradient-echo sequence, and preliminary clinical experience. *Radiology*. 2017;282(2):390–8. <https://doi.org/10.1148/radiol.2016160153>.
- Choi SL, Lee ES, Ko A, et al. Technical success rates and reliability of spin-echo echo-planar imaging (SE-EPI) MR elastography in patients with chronic liver disease or liver cirrhosis. *Eur Radiol*. 2020;30(3):1730–7. <https://doi.org/10.1007/s00330-019-06496-y>.
- Kim D, W, Kim SY, Yoon HM, Kim KW, Byun JH. Comparison of technical failure of MR elastography for measuring liver stiffness between gradient-recalled echo and spin-echo echo-planar imaging: a systematic review and meta-analysis. *J Magn Reson Imaging*. 2020;51(4):1086–102. <https://doi.org/10.1002/jmri.26918>.
- Wagner M, Hectors S, Bane O, et al. Noninvasive prediction of portal pressure with MR elastography and DCE-MRI of the liver and spleen: preliminary results. *J Magn Reson Imaging*. 2018;48:1091–103.
- Glaser KJ, Manduca A, Ehman RL. Review of MR elastography applications and recent developments. *J Magn Reson Imaging*. 2012;36(4):757–74. <https://doi.org/10.1002/jmri.23597>.
- Allen AM, Shah VH, Therneau TM et al. The role of three-dimensional magnetic resonance elastography in the diagnosis of nonalcoholic steatohepatitis in obese patients undergoing bariatric surgery. *Hepatology*. 2020;71(2):510–21. <https://doi.org/10.1002/hep.30483>.
- Loomba R CJ, Wolfson T, et al. . Novel 3D Magnetic Resonance Elastography for the Noninvasive Diagnosis of Advanced Fibrosis in NAFLD: A Prospective Study. *Am J Gastroenterol*. 2016;111(7):986–94. <https://doi.org/10.1038/ajg.2016.65>.

26. Li M, Yang H, Liu Y, Zhang L, Chen J, Deng Y, et al Comparison of the diagnostic performance of 2D and 3D MR elastography in staging liver fibrosis. *Eur Radiol.* 2021;31(12):9468–78. <https://doi.org/10.1007/s00330-021-08053-y>.
27. Forsgren MF, Norén B, Kihlberg J, Dahlqvist Leinhard O, Kechagias S, Lundberg P. Comparing hepatic 2D and 3D magnetic resonance elastography methods in a clinical setting - Initial experiences. *Eur J Radiol Open.* 2015;2:66–70. Epub 20150428. <https://doi.org/10.1016/j.ejro.2015.04.001>. PubMed PMID: 26937438; PMCID: PMC4750624.
28. Morisaka H, Motosugi U, Glaser KJ, Ichikawa S, Ehman RL, Sano K, Ichikawa T, Onishi H. Comparison of diagnostic accuracies of two- and three-dimensional MR elastography of the liver. *J Magn Reson Imaging.* 2017;45(4):1163–70. Epub 20160923. <https://doi.org/10.1002/jmri.25425>. PubMed PMID: 27662640; PMCID: PMC5584543.
29. Qu Y, Middleton MS, Loomba R, Glaser KJ, Chen J, Hooker JC, Wolfson T, Covarrubias Y, Valasek MA, Fowler KJ, Zhang YN, Sy E, Gamst AC, Wang K, Mamidipalli A, Schwimmer JB, Song B, Reeder SB, Yin M, Ehman RL, Sirlin CB. Magnetic resonance elastography biomarkers for detection of histologic alterations in nonalcoholic fatty liver disease in the absence of fibrosis. *Eur Radiol.* 2021;31(11):8408–19. Epub 20210426. <https://doi.org/10.1007/s00330-021-07988-6>. PubMed PMID: 33899143; PMCID: PMC8530863.
30. Shi Y, Xia F, Li QJ, Li JH, Yu B, Li Y, An H, Glaser KJ, Tao S, Ehman RL, Guo QY. Magnetic Resonance Elastography for the Evaluation of Liver Fibrosis in Chronic Hepatitis B and C by Using Both Gradient-Recalled Echo and Spin-Echo Echo Planar Imaging: A Prospective Study. *Am J Gastroenterol.* 2016;111(6):823–33. Epub 20160315. <https://doi.org/10.1038/ajg.2016.56>. PubMed PMID: 26977760.
31. Shi Y QY, Lan GY, et al. . Three-dimensional MR Elastography Depicts Liver Inflammation, Fibrosis, and Portal Hypertension in Chronic Hepatitis B or C. . *Radiology.* 2021;301(1):154–62. <https://doi.org/10.1148/radiol.2021202804>.
32. Wang J, Shan Q, Liu Y, et al. 3D MR elastography of hepatocellular carcinomas as a potential biomarker for predicting tumor recurrence. *J Magn Reson Imaging.* 2019;49(3):719–30. <https://doi.org/10.1002/jmri.26250>.
33. Yin M, Glaser KJ, Talwalkar JA, Chen J, Manduca A, Ehman RL. Hepatic MR elastography: clinical performance in a series of 1377 consecutive examinations. *Radiology.* 2016;278(1):114–24. <https://doi.org/10.1148/radiol.2015142141>.
34. Dzyubak B, Venkatesh SK, Manduca A, Glaser KJ, Ehman RL. Automated liver elasticity calculation for MR elastography. *J Magn Reson Imaging.* 2016;43(5):1055–63. <https://doi.org/10.1002/jmri.25072>.
35. Yin M, Glaser KJ, Manduca A, Mounajjed T, Malhi H, Simonetto DA, Wang R, Yang L, Mao SA, Glorioso JM, Elgilani FM, Ward CJ, Harris PC, Nyberg SL, Shah VH, Ehman RL. Distinguishing between Hepatic Inflammation and Fibrosis with MR Elastography. *Radiology.* 2017;284(3):694–705. Epub 20170127. <https://doi.org/10.1148/radiol.2017160622>. PubMed PMID: 28128707; PMCID: PMC5529282.
36. Bedossa P PT. An algorithm for the grading of activity in chronic hepatitis C. The METAVIR Cooperative Study Group. *Hepatology.* 1996;24(2):289–93. <https://doi.org/10.1002/hep.510240201>.
37. Bedossa P, Poynard T An algorithm for the grading of activity in chronic hepatitis C. The METAVIR Cooperative Study Group. *Hepatology.* 1996;24(2):289–93. <https://doi.org/10.1002/hep.510240201>.
38. Puri P SAPSdc. Nonalcoholic fatty liver disease: Definitions, risk factors, and workup. . *Clin Liver Dis (Hoboken).* 2012;1(1):99–103. <https://doi.org/10.1002/cld.81>.
39. Calvaruso V, Burroughs AK, Standish R, Manousou P, Grillo F, Leandro G, Maimone S, Pleguezuelo M, Xirouchakis I, Guerrini GP, Patch D, Yu D, O'Beirne J, Dhillon AP. Computer-assisted image analysis of liver collagen: relationship to Ishak scoring and hepatic venous pressure gradient. *Hepatology.* 2009;49(4):1236–44. Epub 2009/01/13. <https://doi.org/10.1002/hep.22745>. PubMed PMID: 19133646.
40. Kennedy P WM, Castéra L, Hong CW, Johnson CL, Sirlin CB, Taouli B. . Quantitative Elastography Methods in Liver Disease: Current Evidence and Future Directions. . *Radiology.* 2018 286(3):738–63. <https://doi.org/10.1148/radiol.2018170601>.
41. Besa C, Wagner M, Lo G, Gordic S, Chatterji M, Kennedy P, Stueck A, Thung S, Babb J, Smith A, Taouli B. Detection of liver fibrosis using qualitative and quantitative MR elastography compared to liver surface nodularity measurement, gadoxetic acid uptake, and serum markers. *J Magn Reson Imaging.* 2018;47(6):1552–61. Epub 20171128. <https://doi.org/10.1002/jmri.25911>. PubMed PMID: 29193508.
42. Li M YH, Liu Y, Zhang L, Chen J, Deng Y, et al. . Comparison of the diagnostic performance of 2D and 3D MR elastography in staging liver fibrosis. *Eur Radiol.* 2021;31(12):9468–78. <https://doi.org/10.1007/s00330-021-08053-y>.
43. Wang Y, Ganger DR, Levitsky J, Sternick LA, McCarthy RJ, Chen ZE, Fasanati CW, Bolster B, Shah S, Zuehlsdorff S, Omary RA, Ehman RL, Miller FH. Assessment of chronic hepatitis and fibrosis: comparison of MR elastography and diffusion-weighted imaging. *AJR Am J Roentgenol.* 2011;196(3):553–61. <https://doi.org/10.2214/ajr.10.4580>. PubMed PMID: 21343496; PMCID: PMC3093963.
44. Serai SD, Yin M, Wang H, Ehman RL, Podberesky DJ. Cross-vendor validation of liver magnetic resonance elastography. *Abdom Imaging.* 2015;40(4):789–94. <https://doi.org/10.1007/s00261-014-0282-y>. PubMed PMID: 25476489; PMCID: PMC4523216.

Publisher's Note Springer Nature remains neutral with regard to jurisdictional claims in published maps and institutional affiliations.

Springer Nature or its licensor (e.g. a society or other partner) holds exclusive rights to this article under a publishing agreement with the author(s) or other rightsholder(s); author self-archiving of the accepted manuscript version of this article is solely governed by the terms of such publishing agreement and applicable law.

Authors and Affiliations

Enamul H. Bhuiyan^{1,2} · Efe Ozkaya^{1,2} · Paul Kennedy^{1,2} · Juan Lloret Del Hoyo^{2,3} · Bassam El Achkar² · Swan Thung⁴ · Sara Lewis^{1,2} · Octavia Bane^{1,2} · Bachir Taouli^{1,2} 

✉ Bachir Taouli
bachir.taouli@mountsinai.org

Enamul H. Bhuiyan
enamul.bhuiyan@mountsinai.org

Efe Ozkaya
efe.ozkaya@mountsinai.org

Paul Kennedy
paul.kennedy@bsci.com

Juan Lloret Del Hoyo
jllorethoyo@gmail.com

Bassam El Achkar
bassam.elachkar@mountsinai.org

Swan Thung
swan.thung@mountsinai.org

Sara Lewis
sara.lewis@mountsinai.org

Octavia Bane
octavia.bane@mountsinai.org

¹ BioMedical Engineering and Imaging Institute (BMEII), Icahn School of Medicine at Mount Sinai, New York, NY, USA

² Department of Diagnostic, Molecular and Interventional Radiology, Icahn School of Medicine at Mount Sinai, New York, NY, USA

³ Department of Radiology, NYU Grossman School of Medicine, New York, NY, USA

⁴ Department of Pathology, Molecular and Cell-Based Medicine, Icahn School of Medicine at Mount Sinai, New York, NY, USA